Real-time dynamics of clusters. III. I_2Ne_n ($n=2$–4), picosecond fragmentation, and evaporation

M. Gutmann,[a] D. M. Willberg, and A. H. Zewail
Arthur Amos Noyes Laboratory of Chemical Physics,[b] California Institute of Technology, Pasadena, California 91125

(Received 1 July 1992; accepted 25 August 1992)

In this paper (III) we report real-time studies of the picosecond dynamics of iodine in Ne clusters $I_2^*Ne_n(n = 2–4) \rightarrow I_2^* + n\text{Ne}$. The results are discussed in relation to vibrational predissociation (VP), basic to the I_2X systems, and to the onset of intramolecular vibrational-energy redistribution (IVR). The latter process, which is a precursor for the evaporation of the host atoms or for further fragmentation, is found to be increasingly effective as the cluster size increases; low-energy van der Waals modes act as the accepting (bath) modes. The reaction dynamics for I_2Ne_2 are examined and quantitatively compared to a simple model which describes the dynamics as consecutive bond breaking. On this basis, it is concluded that the onset of energy redistribution is observed in I_2Ne_2. Comparison of I_2Ne and I_2Ne_2 to larger clusters ($n=3,4$) is accomplished by introducing an overall effective reaction rate. From measurements of the rates and their dependence on v_i', the initial quantum number of the I_2 stretch, we are able to examine the dynamics of direct fragmentation and evaporation, and compare with theory.

I. INTRODUCTION

The reaction dynamics of size-selected van der Waals (vdW) clusters form a basis for understanding the interplay between intramolecular vibrational-energy redistribution (IVR) and the direct fragmentation by vibrational predissociation (VP). For the case at hand, halogen–rare gas clusters, there are two interesting regimes for the dynamics which are determined by the effective size of the cluster. For small clusters, the "small-molecule" description of the dynamics may apply as in the case of I_2He, I_2Ne, and I_2Ar ($n=1$), discussed in Papers (I)[1] and (II).[2] In this case, the dynamics of VP are governed only by the coupling between the initially prepared metastable bound state and the final dissociation continuum (see Fig. 1).

For the larger clusters, the density of states plays an important role in the dynamics, perhaps reaching the statistical limit of the "large-molecule" case. The initially prepared state in this case couples not only to the mode(s) of the reactive coordinate(s), but also to nonreactive "bath modes" whose number increases with n. The transition from one regime to the other is interesting to explore, both theoretically and experimentally.

An important question concerning the larger clusters ($n>1$) relates to the mechanism: Do the rare gas atoms directly break one at a time (a sequential mechanism), or do they indirectly fragment following energy redistribution? And if indirect fragmentation is the pathway, does it occur by VP or evaporation? Consider, for example, I_2Ne_2. The two possibilities for direct fragmentation by VP are

$$I_2^*Ne_2(v_i') \rightarrow I_2^*(v_i'-2) + 2\text{Ne} \tag{1}$$

or

$$I_2^*Ne_2(v_i') \rightarrow I_2^*Ne(v_i'-1) + \text{Ne}, \tag{2a}$$

$$I_2^*Ne(v_i'-1) \rightarrow I_2^*(v_i'-2) + \text{Ne}, \tag{2b}$$

where v_i' is the vibrational quantum number of the initial iodine stretch. These direct pathways in Eqs. (1) and (2) contrast a path in which energy is dissipated to the modes of the surrounding atoms/I_2 cluster. Because of the presence of the two neons, energy redistribution from the I_2 stretch to nonreactive modes could compete with direct VP, leading to a new channel

$$I_2^*Ne_2(v_i') \rightarrow I_2^*Ne_2^\ddagger(v_i'-1). \tag{3}$$

The thermally excited cluster (denoted by ‡) may then lose the Ne atoms by VP or by evaporation. For the latter, perhaps, statistical theories could be used to calculate the rates.

Frequency domain studies of electronically excited neutral dihalogen rare gas clusters have been carried out on the systems I_2He_n,[3] I_2Ne_n,[4] Br_2Ne_n,[5] Cl_2Ne_n,[6] and $IClNe_n$,[7] where $n>1$. To resolve the dynamics in real-time and separate the different channels, the state-to-state rates of VP and vibrational relaxation must be measured. As shown in (I) and (II), linewidth measurements can give an upper limit of the rate for the first step of the dynamics. A goal which can, in principle, be reached by the time-resolved studies is the determination of the rates of the individual steps by probing the reaction intermediates directly.

This paper focuses on studies in real-time of the state-to-state rates in I_2Ne_n ($n=2,3,4$) and extends the earlier results reported in (I) and (II). To probe the dynamics, we use the following pump–probe/molecular beam methodology:[8] A picosecond pump pulse prepares the cluster under consideration in a well-defined vibrational state v_i' of the I_2 stretch mode (in the electronic B state). The decay of this metastable state into the final dissociation continuum,

$$I_2^*Ne_n(v_i') \rightarrow I_2^*(v_f'=v_i'-m) + n\text{Ne} \tag{4}$$

[a]Deutsche Forschungsgemeinschaft post-doctoral fellow from Germany.
[b]Contribution No. 8639.

 0021-9606/92/238048-12$006.00

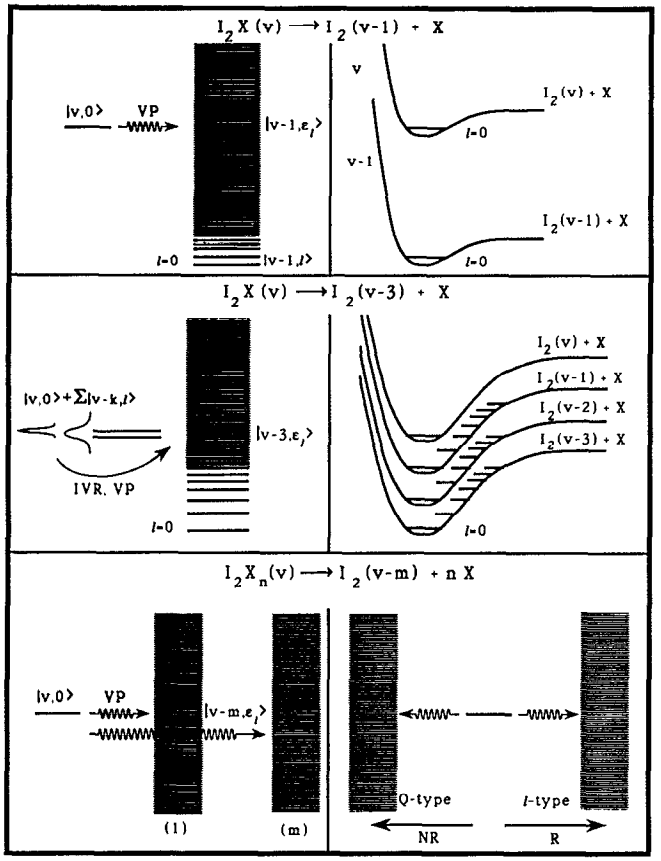

FIG. 1. Schematic showing the dynamics of VP and IVR in different cluster limits. The top panels are typical of the I_2X (X=Ne) system where the energy of one quantum of the I_2 stretch is larger than the vdW binding energy. The middle panels show the reverse case where intermediate discrete states may give rise to IVR processes; the panel on the left describes the dependence of IVR on the initial preparation (see the text). Finally, the panels at the bottom describe IVR and VP in larger clusters where two types of modes (reactive, *l*, and nonreactive, *Q*) are available.

is followed by monitoring the I_2 final state, using a temporally delayed picosecond probe pulse in resonance with the final quantum state. This way, the absolute rates are measured for the different channels [denoted by m in Eq. (4)] of each cluster, and also their dependence on the initial quantum number of the I_2 stretch vibration. For I_2Ne_2, we discuss detailed results of the m channels for the selected states v_i', and we propose a mechanism for the reaction. For clusters with larger n, we identify the effective reaction rate which critically depends on n and v_i'.

Lineberger's group[9] has elegantly demonstrated the dependence of the dynamics in the $I_2^-(CO_2)_n$ and related systems on the cluster size using these pump–probe methods. There are also theoretical models by Amar and Berne[10] which elucidate the mechanism of the fragmentation processes for different n. The size selection in these experiments was made using mass resolution since the system under consideration has a net charge. For neutral clusters, the selection is made using spectroscopic resolution as discussed below.

From the pioneering work of Levy and co-workers[4] on I_2Ne_n ($n=1$–7), the spectroscopic shifts are known quite accurately. Furthermore, for $n>1$, the product state distribution of nascent I_2 is characterized by different vibrational states, v_f'. As one quantum of the I_2 stretch vibration corresponds to $\sim 100\ cm^{-1}$ and the vdW binding energy in I_2Ne is $\sim 66\ cm^{-1}$ (D_0),[11] the first observed channel for nascent I_2 from I_2Ne_2 is $m=2$. The $m=3$ channel is of comparable efficiency for $v_i' \sim 20$ (Ref. 4). In I_2Ne_3, the most efficient channel is not, as would be expected by energetic reasoning, the $m=3$ channel (which was still observed), but the higher $m=4$ channel. Even $m=5$ was observed. The larger n becomes, the more preferable the higher channels with $m>n$ are. From this behavior, it was concluded that VP becomes less efficient as the cluster size increases.[4]

This paper is organized as follows: In Sec. II we give a very brief description of the experimental methodology; for more details see (I) and (II). In Sec. III we give an account of the results and discuss them in relation to the mechanism of fragmentation and evaporation. Comparisons with recent theoretical calculations are also discussed. We conclude this contribution in Sec. IV.

II. EXPERIMENT

A. Apparatus

The picosecond laser system and the molecular beam apparatus used in these experiments were described in (I) and (II). Here the experiments were performed by selectively exciting the cluster under consideration from the ground state $X(v''=0)$ to the desired $B(v_i')$ state by tuning the pump laser pulse. Similarly, the probe was tuned to the transition of interest and laser-induced fluorescence was detected as a function of the delay between the pump and probe pulses. The pump pulse energy was $\sim 5\ \mu J$, and that of the probe pulse, after frequency doubling, was $\sim 0.2\ \mu J$. Both pulses had approximately Gaussian profiles with a bandwidth (FWHM) of $\sim 3\ cm^{-1}$. The cross-correlation measured between both laser pulses (the probe pulse was not frequency doubled) was fitted to a Gaussian function with a width (FWHM) of 40 ± 3 ps over the entire frequency range used in these studies.

Selective excitation of a given cluster was possible because of the relatively large spectral shift between the $B(v_i') \leftarrow X(v''=0)$ transition of I_2Ne_n and I_2Ne_{n-1}. The shift is larger than the bandwidth of our laser pulses; for $n<7$, the shift, for I_2Ne_n, is approximately $n\times 6.5\ cm^{-1}$ ($v_i'=20$).[4,12]

The I_2Ne_n clusters were formed by seeding a free jet expansion of Ne (99.996% purity, Spectra Gases) with iodine (99.999% purity, Aldrich). The backing pressure was typically about 75 psig and X/D was ~ 75 (X is the distance downstream from the nozzle). For the pulsed solenoid valve used here, the diameter was 150 μm and the repetition rate was 100 Hz.

B. Data analysis

In order to obtain the rates of the different steps involved, care had to be taken in fitting the data to a single or double exponential rise. The fitting routine we used[13] was

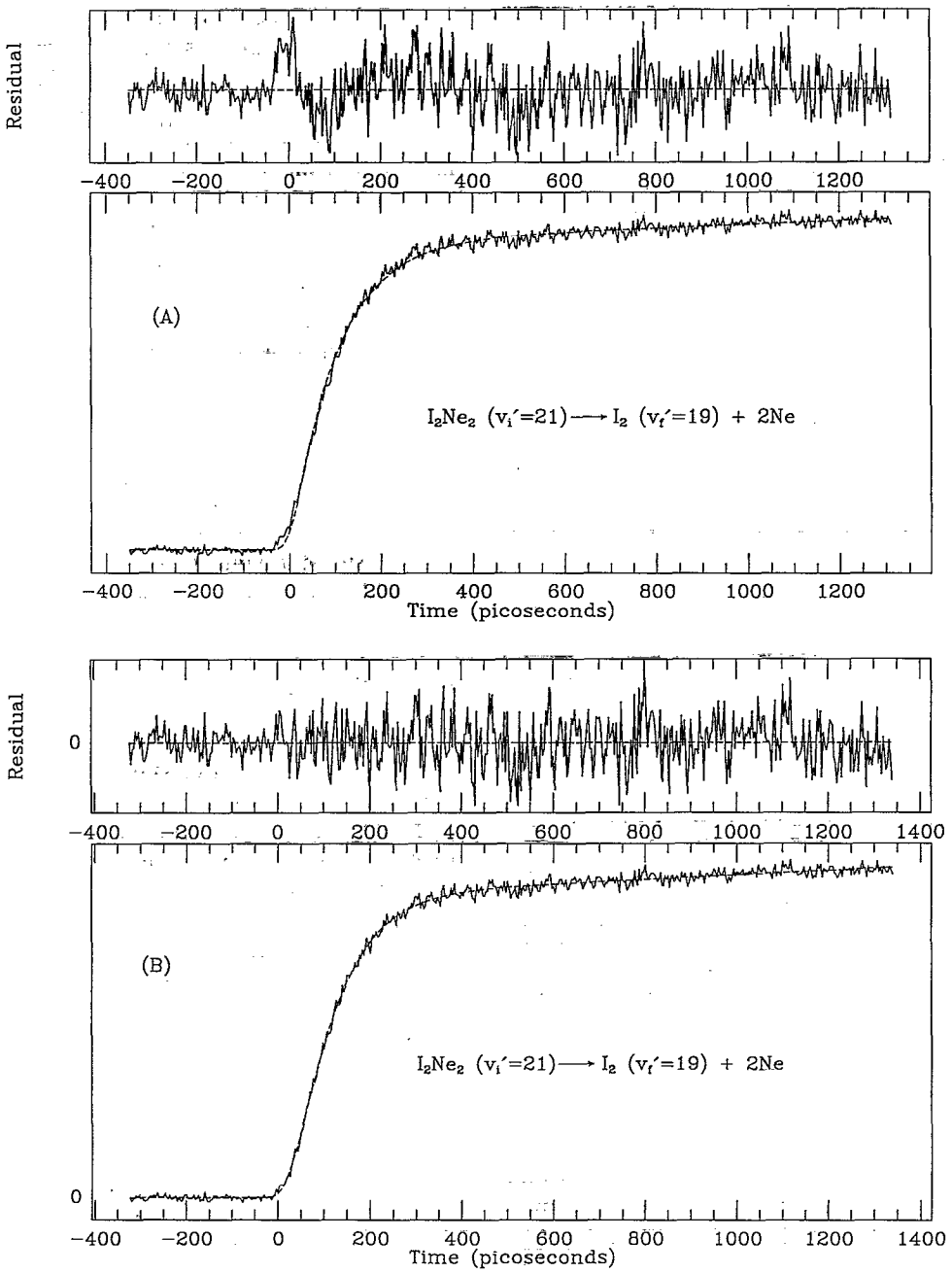

FIG. 2. An experimental transient of I_2Ne_2 ($v_i' = 21$, $v_f' = 19$) together with fits to a single exponential rise convoluted with a 40 ps system response (A) and a double exponential rise convoluted with a 40 ps system response (B). The robustness of these fits are discussed in the text.

based on a nonlinear-least-squares-fit Marquardt algorithm.[14] The fitting parameters contained the inverse rate constant(s), the zero of time (T_0), the baseline height, the signal intensity, and the FWHM of the cross correlation (Δ). Depending on the individual transients, we also took into account the possible existence of long time signal sloping at the asymptote. The parameter Δ was fixed at the measured value and the other parameters were obtained from the fits. As these observed slopes (due to slight misalignment of the pump and probe overlap over very long distances, i.e., very long times) varied randomly within groups of scans of the same v_i', they were not believed to reveal any additional dynamical features.

For I_2Ne_2, the fits to single exponential rise functions led to consistent rates within each group of scans, but as shown in Fig. 2, the results fitted the actual transients poorly (see discussion in Sec. III). Forcing the fits to single exponentials showed only little changes with parameters. For example, varying Δ from 27 to 53 ps, the inverse rate constant τ was fitted between 98 and 104 ps and T_0 shifted within 2.5 ps for these Δ variations. However, the residuals showed systematic deviations of the transient from a single

exponential behavior; T_0 was shifted to rather high values relative to the origin of the experimental transient (more than 25 ps) and the single exponential rate values lacked a physically sound interpretation [see Fig. 2(A) and Sec. III].

Fits to double exponential rise functions, however, reproduced the measured transients well. The double exponential fits, which showed good signal-to-noise ratios and essentially no pronounced slopes at long times, yielded two different rate constants whose values could be interpreted in line with what is known about the I_2Ne ($n=1$) results and the theoretical predictions. When the transients exhibited poor signal-to-noise ratio and/or considerable slopes, the deduced rates approached each other in value. As expected, the uniqueness of the fits was eroded. There are four reasons which support the exclusion of fits exhibiting nearly identical rate values for a two step reaction:

(i) The statistical correlation between both inverse rate constants was very high compared to those fits that showed different inverse rate constants;

(ii) the calculated deviations of the fitted inverse rate constants were very large ($>100\%$) compared to those fits with different rates;

(iii) the fitted VP time for the second step deviates strongly from the corresponding VP time measured for I_2Ne and reported in Paper (I) (see the discussion in Sec. III); and

(iv) theoretical calculations predict that the first step of the consecutive bond breakage is much faster than the second one (see the discussion in Sec. III).

In order to show that the double exponential fits are robust with respect to changes in the fixed parameters (i.e., Δ), we chose two transients and varied Δ consistently between 27 and 53 ps (note that the measured cross correlation gives $\Delta=40$ ps). A double exponential fit to the transient shown in Fig. 2(B) ($v_i'=21$) using $\Delta=40$ ps gave the two inverse rate constants $\tau_1=42$ ps and $\tau_2=80$ ps. Varying Δ led to changes in T_0 between -3 and $+4$ ps, i.e., only about 10% of Δ. τ_1 was between 33 ps ($\Delta=53$ ps) and 49 ps ($\Delta=27$ ps), a quite acceptable range, particularly when considering that τ_1 is close to the width of the cross correlation. τ_2 was between 75 ps ($\Delta=27$ ps) and 84 ps ($\Delta=53$ ps), well within the experimental error bar and within 10% of the above 80 ps value. As can be seen from Fig. 2(B), this transient shows an upward slope, so fixing the slope parameter to a value of zero should give an unreasonable fit. This is indeed the case, as doing so led to $\tau_1=15$ ps and $\tau_2=115$ ps.

In order to check for any effects of the slope parameter on the fitted inverse rates, we performed another check on a transient showing hardly a noticeable slope. This transient belonged to the $v_i'=17$ group. Inclusion of the slope parameter and setting $\Delta=40$ ps led to values of $\tau_1=82$ ps and $\tau_2=155$ ps. Varying Δ as above and retaining the slope parameter led to T_0 changes between -2 and $+3$ ps, τ_1 between 75 ps ($\Delta=53$ ps) and 86 ps ($\Delta=27$ ps), and τ_2 between 160 ps ($\Delta=27$ ps) and 165 ps ($\Delta=53$ ps). The same procedure, setting the slope parameter to zero, gave us the following results: With $\Delta=40$ ps, T_0 shifted $+1$ ps and the inverse rate constants were $\tau_1=77$ ps and $\tau_2=162$ ps. Varying Δ led to T_0 shifts between -1 and $+3$ ps, τ_1 between 72 ps ($\Delta=53$ ps) and 80 ps ($\Delta=27$ ps), and τ_2 between 160 ps ($\Delta=27$ ps) and 165 ps ($\Delta=53$ ps). All these values are well within our experimental error bars and demonstrate the reliability of the accepted double exponential fits.

For the larger clusters ($n=3$ and $n=4$) we fitted all of our transients to an effective single exponential rise function as discussed in Sec. III. Even though these results did not fit the actual transients well (the higher n the larger the discrepancy of the simulation), they consistently provided an effective rate and showed a late onset (on the order of 30 ps) of the rise in comparison to the experimental transients. The fitted inverse rate constants were consistent and stable against variations in Δ as described above.

III. RESULTS AND DISCUSSION

Figure 3 shows some of the transients we obtained for the I_2Ne_n ($n=1,2,3,4$) clusters. Transients are presented for I_2Ne ($v_i'=17,19,21$),[1] Fig. 3(A); I_2Ne_2 ($v_i'=17,19,21$; $m=2$ channel), Fig. 3(B); I_2Ne_3 ($v_i'=19,21,23$; $m=4$ channel), Fig. 3(C); and I_2Ne_4 ($v_i'=22$, $m=5$ channel), Fig. 3(D). By visual inspection of these transients, it is observed that the temporal behavior within the same cluster size changes significantly with v_i'. The measured rate increases as v_i' increases for all clusters studied. Furthermore, it can also be seen that the effective rates (*vide infra*) decrease with increasing cluster size for each vibrational level v_i' studied. The latter observation would appear to be in contradiction with the lifetime deduced from linewidth measurements;[4] the authors reported a shortening of the lifetime when going from I_2Ne to I_2Ne_2 (cp. Table IV in Ref. 4).

The above-mentioned contradiction, however, is easily resolved (*vide infra*) when one considers the fact that rates deduced from linewidth measurements, if homogeneous, only reflect the first step of a complicated multistep process, e.g., the fast component in a biexponential process. Such complications in large clusters have been discussed by Levy and co-workers.[4]

The following conclusions can be drawn from the time-resolved studies:

(1) The overall rates (not only the first step) depend strongly on v_i'.

(2) The overall rates slow down with increasing cluster size in I_2Ne_n.

(3) The dynamics in larger clusters involve multistep processes which cannot be resolved by linewidth measurements.

In what follows, we shall consider the process of direct fragmentation and focus on the I_2Ne_2 system. We then shall consider this and the larger clusters to address the issue of direct fragmentation and energy redistribution as n increases.

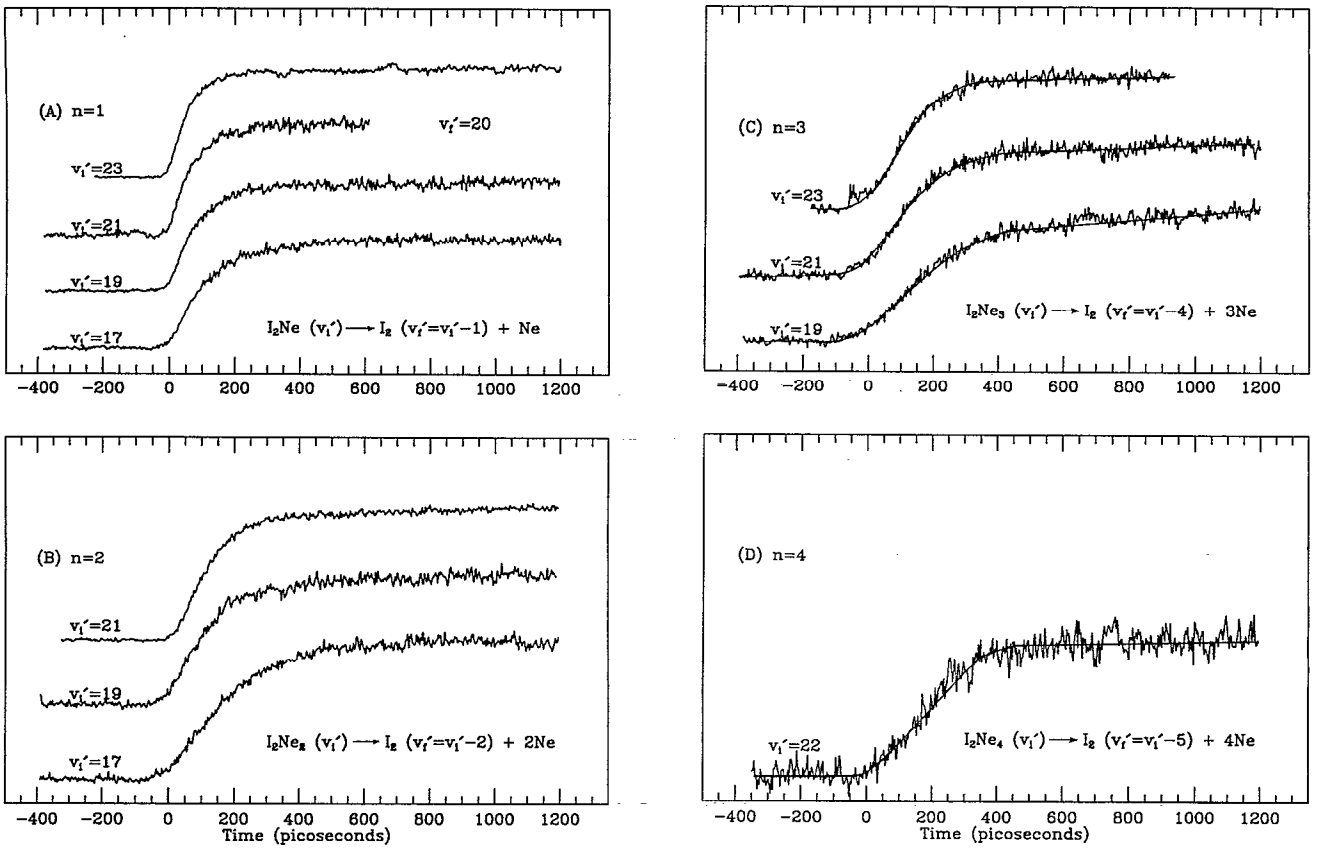

FIG. 3. Typical I_2Ne_n transients for various values of v_i': (A) transients for $n=1$, (B) transients for $n=2$, (C) transients for $n=3$, and (D) shows a transient recorded for a $n=4$ cluster.

A. Direct fragmentation, redistribution, and evaporation

Sequential bond breaking in a cluster can be first considered by assuming a local mode description of the reaction coordinate. With this model, Kellman derived propensity rules of VP in I_2Ne_n clusters.[15] If bond breaking occurs mainly sequentially, the VP process is described within the framework of this model simply by neglecting intermode coupling. Kellman separated the Hamiltonian as follows:

$$H=H_0+V+V_{\rm mc}\,, \tag{5}$$

where

$$V=\sum_{i=1}^{n} V(r,R_i). \tag{6}$$

H_0 is the zero-order local mode Hamiltonian. $V_{\rm mc}$ gives the correction to the local mode approximation, i.e., the correlation effects due to mode coupling. The coupling (V) is between the I_2 stretch mode along the intramolecular coordinate r and the vdW stretch modes along the "intermolecular" reaction coordinates R_i.

The zero-order eigenfunctions of H_0 are the bound states $|v',l_{i1}'(1),l_{i2}'(2),...,l_{in}'(n)\rangle$, where v' denotes the quantum number of the I_2 stretch mode and $l_{ik}'(k)$ represents the local vdW vibrational state i with respect to the kth Ne atom (it essentially denotes the vdW stretch mode, possibly including bending modes). If correlation is included (e.g., by applying perturbation techniques), the corresponding wave function, according to its leading term, is written as[15] $|\Psi[v',l_{i1}'(1),...,l_{in}'(n)]\rangle$.

For a sequential process, a change of one quantum in the I_2 stretch mode at a time will be considered. For the first step, one such quantum has sufficient energy to dissociate one Ne atom, assuming that the binding energy of n Ne atoms ($n<7$, see Ref. 4) is n times as large as that of one Ne atom. In the local mode picture, the metastable bound state $|\Psi[v_i',l_{i1}'(1),\cdots l_{in}'(n)]\rangle$ can couple to n zero-order continua:

$$|\Psi[v_i'-1,\epsilon'(1),l_{j1}'(2),...,l_{jn}'(n)]\rangle,$$
$$|\Psi[v_i'-1,l_{k1}'(1),\epsilon'(2),l_{k3}'(3),...,l_{kn}'(n)]\rangle,...,$$
$$|\Psi[v_i'-1,l_{m1}'(1),...,l_{n-1}'(n-1)\epsilon'(n)]\rangle,$$

where ϵ' denotes the kinetic energy of the recoiling fragments, i.e., $I_2Ne_{n-1}+Ne$ (see Fig. 1).

There is also the possibility of nonreactive energy redistribution to the cluster modes which results in heating. The redistribution can lead to VP or to evaporation of the Ne atoms, (probably) by a statistical energy channeling to the reaction coordinate. In order to avoid dissociation, the energy has to be shared by the different cluster modes, below the dissociation energy. As the coupling operator is assumed to be a one particle operator, correlated bound wave functions have to be considered to allow for excitation of more than one local mode. The coupling for nonreactive energy redistribution is then between the initial

metastable state and the bound levels. In a golden rule description, the rate for nonreactive energy redistribution from I_2 to the cluster modes in I_2Ne_n can be written as $k^r(n|v_i',\{l'\})$

$$\propto |\langle\Psi[v_i',l_{i1}'(1),\ldots,l_{in}'(n)]|V \times |\Psi(v_j',l_{k1}'(1),\ldots,l_{kn}'(n)]\rangle|^2\rho, \quad (7)$$

where ρ is the relevant density of states.[16] v_i' (v_j') denotes the initially excited (final) I_2 stretch level and $\{l'\}$ describes all vdW vibrations involved.

In writing Eq. (7), we have assumed that IVR is not restricted,[17] i.e., dissipative, and that coherence effects are absent. This has been shown not to be the case even for large molecules,[18] but perhaps is justified here, if we assume that the low-energy modes of the clusters form a quasicontinuum (see Fig. 1). This "kinetic limit description" of IVR has been discussed elsewhere.[19]

The rate for the direct one-quantum VP, $I_2Ne_n \rightarrow I_2Ne_{n-1}$, from the v_i' state can now be expressed as follows:[20]

$$k^{VP}(n,n-1|v_i',\{l'\}) \propto |\langle\Psi[v_i',l_{i1}'(1),\ldots,l_{in}'(n))|V|\Psi(v_i'-1,\epsilon'(1),l_{k2}'(2),\ldots,l_n'(n))\rangle|^2+\cdots + |\langle\Psi(v_i',l_{i1}'(1),\ldots,l_{in}'(n))|V|\Psi(v_i'-1,l_{m1}'(1),\ldots,l_{n-1}'(n-1),\epsilon'(n)]\rangle|^2. \quad (8)$$

Assuming that correlation effects are negligible (i.e., a pure local mode picture), Eq. (8) reduces to

$$k^{VP}(n,n-1|v_i',\{l'\}) \propto |\langle v_i',l_{i1}'(1)|V(r,R_1)|v_i'-1,\epsilon'(1)\rangle|^2+\cdots+|\langle v_i',l_n'(n)|V(r,R_n)|v_i'-1,\epsilon'(n)\rangle|^2. \quad (9)$$

If the initial state is prepared such that all vdW vibrations are identical [e.g., in the ground vibrational state $l_{ik}'(k) = 0$], Eq. (9) can be simplified to give

$$k^{VP}(n,n-1|v_i',l_1') = nk^{VP}(1,0|v_i',l_1') \propto n|\langle v_i',l_1'(1)|V(r,R_1)|v_i'-1,\epsilon'(1)\rangle|^2. \quad (10)$$

As reported in (I), $k^{VP}(1,0|v_i',l_1')$ refers to the rate constant of VP in I_2Ne. If the nonreactive channel competes with VP, the first step of the reaction involves a total rate given by

$$K(n|v_i',\{l'\}) = k^{VP}(n,n-1|v_i',\{l'\}) + k^r(n|v_i',\{l'\}). \quad (11)$$

Although some approximations have been invoked in obtaining Eq. (10), it leads to a simple concept concerning the first step of VP: If no nonreactive energy redistribution is present, the VP time for the first step will roughly scale as $1/n$ that of the corresponding VP process in I_2Ne. Thus by comparing the rate of the first step of VP in I_2Ne_n with n times that of the corresponding VP rate in I_2Ne, one should obtain an estimate of the importance of the nonreactive channel. In the quasiclassical trajectory calculations of Delgado-Barrio and co-workers,[21] discussed below, the difference between K and k^{VP} is attributed to IVR, the energy redistribution that describes k^r. It should be noted that in nonreactive energy dissipation, it is possible to have energy redistribution maintaining the total energy of the I_2X_n systems constant (IVR) or lowering the I_2 energy with the solvent acquiring kinetic energy (vibrational relaxation (VR), in this case equivalent to VP).

The above discussion considered the two initial pathways: direct coupling to the reaction coordinates or dissociation continua (or to modes that possess a component along the reaction coordinates) and coupling to modes that are not part of the reaction coordinates or dissociation continua. The latter energy redistribution is IVR, and if IVR is involved, the energy transferred to these nonreactive modes can still be channelled into the reaction coordinates and we have IVR, possibly preceding "statistical evaporation." Also, IVR can precede another VP fragmentation as discussed by Semmes *et al.*[22] (see also Fig. 1). Finally, we notice that in Eq. (8), if all n atoms are simultaneously fragmented by VP, the I_2 vibrational energy must be changed by at least n quanta at once, a highly improbable process, certainly for harmonic and even anharmonic systems. That is why in these VP systems, unlike chemical bond breakage,[23] the propensity is toward a sequential mechanism.

In order to obtain the dynamics of VP for the first step let us now consider the first member of this cluster family, I_2Ne_2.

B. The I_2Ne_2 cluster

In this case, the scheme for direct VP and energy redistribution can be written as

$$I_2^*Ne_2(v_i') \xrightarrow{k_1^{VP}} I_2^*Ne(v_i'-1) \xrightarrow{k_2^{VP}} I_2^*(v_i'-2) \quad m=2 \text{ channel} \quad (12a)$$

$$\Big\downarrow k^r$$

$$I_2^*Ne_2^{\#}(v_i'-1) \xrightarrow{k_1^{VP}} I_2^*Ne(v_i'-2) \xrightarrow{k_2^{VP}} I_2^*(v_i'-3) \quad m=3 \text{ channel} \quad (12b)$$

$$\Big\downarrow \langle k\rangle$$

Evaporation

Here the redistribution leads to a "hot" cluster and IVR precedes VP for the $m=3$ channel. The number of m channels in this scheme should be sufficient as the yield of higher channels is negligible.[4] Note that the fact that we detect I_2 in $m=3$ for I_2Ne_2 indicates that direct VP [Eq. (12a)], which involves the expected two quanta change for two neon atoms, must not be the only channel; k^r is also significant, as discussed below.

According to Eq. (12a), the transient buildup of I_2 from I_2Ne_2 should exhibit a biexponential behavior, and for the $m=2$ channel this buildup is simply given by

TABLE I. The rates and time constants for the I_2Ne_2 system: $I_2Ne_2(v_i') \rightarrow I_2(v_f' = v_i' - 2) + 2\,Ne$; $m=2$.[a]

v_i'	$\tau_0/2$ (ps)[b]	τ_1 (ps)	τ_2 (ps)	k_1 ($10^9 s^{-1}$)	k_2 ($10^9 s^{-1}$)
17	63	84 ± 8	165 ± 12	12 ± 2	6 ± 1
18	54	65 ± 5	139 ± 9	15 ± 2	7 ± 1
19	44	47 ± 4	97 ± 4	21 ± 2	10 ± 1
20	39	41 ± 2	91 ± 4	24 ± 2	11 ± 1
21	35	38 ± 5	86 ± 5	26 ± 4	12 ± 1
22	29	23 ± 3	76 ± 5	43 ± 6	13 ± 1
23	27	19 ± 3	44 ± 5	53 ± 9	23 ± 3

[a]The specific values reported for τ_1 and τ_2 are the averages measured for a number of transients; the reported errors are one standard deviation.
[b]These are half the vibrational predissociation lifetimes for $I_2Ne(v_i')$, reported in Paper (I); see the text for further explanation.

TABLE II. A comparison of the measured rate constants with those predicted by the model described in the text.

v_i'	k_1 ($10^9 s^{-1}$)	k_1^c ($10^9 s^{-1}$)[a]	k_2 ($10^9 s^{-1}$)	k_2^c ($10^9 s^{-1}$)[a]
17	12±2	16	6±1	6
18	15±2	19	7±1	8
19	21±2	23	10±1	9
20	24±2	26	11±1	11
21	26±4	29	12±1	13
22	43±6	34	13±1	14
23	53±9	37	23±3	17

[a]k_1^c is calculated by Eq. (10) using the results for VP of I_2Ne from (I); $k_1^c(v)=2k_0(v)$. k_2^c is derived from the results of (I); $k_2^c(v)=k_0(v-1)$. For details, see the text.

$$\text{Signal}(t) \propto \left\{1-\frac{1}{k_2^{VP}-K_1}\left[k_2^{VP}\exp(-K_1 t)-K_1 \times\exp(-k_2^{VP}t)\right]\right\}, \tag{13}$$

where $K_1=k_1^{VP}+k^r$. If the simple relation in Eq. (10) holds with $k^r=0$, then $K_1=k_1^{VP}=2k_0^{VP}(1)$, where $k_0^{VP}(1)$ refers to the corresponding VP time of I_2Ne reported in (I). To obtain the rate constants of both steps, it is important to achieve experimental data with a high signal-to-noise ratio (see Sec. II).

Figure 2 shows a representative transient ($v_i' = 21$) for the $m=2$ channel of I_2Ne_2, fitted to a single exponential rise (A) and to a double exponential rise (B). As discussed in Sec. II, a comparison of these fits shows that a one-step mechanism (single exponential) is not appropriate for describing the dynamics of VP in this system. The single exponential fit in Fig. 2(A) gives $\tau=101$ ps. The double exponential fit is in better accord with the experimental transient and gives $\tau_1=42$ ps and $\tau_2=80$ ps. Similar comparisons for all of our experimental transients ($v_i' = 17$–21) which exhibit good signal-to-noise ratios confirm this observation; the results are shown in Table I. The fits for $v_i' > 21$ did not prove to be very reliable due to the fact that the time constant of the first step is considerably shorter than the measured cross-correlation width (see Sec. II). It is concluded that the mechanism of VP in I_2Ne_2 involves at least a two step process and sequential bond breaking is dominant.

In Table I the results for various v_i' values are shown and in Table II these values are compared with the predictions of the model. The expected rate constant for the first step is $2k_0^{VP}(1)$ (for $v_f' = v_i' - 1$) and for the second step it is $k_0^{VP}(1)$ (for $v_f' = v_i' - 2$). The tabulated rate constants of $2k_0^{VP}(1)$ (for v_i') and $k_0^{VP}(1)$ (for $v_i' - 1$) are derived according to the sequential bond breaking mechanism [Eq. (10) for step 1, and VP of I_2Ne from $v_i' - 1$ for step 2], using the values reported in (I) for I_2Ne ($n=1$).

From Table II, it can be seen that the simple considerations leading to Eq. (10) appear to be in line with these results; however, for $v_i' = 18$, a slight (and for $v_i' = 17$, a significant) slow down of the first step is observed. The fitted rate constants of the second step agree fairly well with the rates measured for I_2Ne. (It should be noted that in comparing the time constants of the second step with the values reported in (I), v_i' must be stepped down by one, as predicted from the above analysis). A comparison of these findings is shown in Fig. 4. The agreement, especially for $v_i' = 19$–21, is rather good.

There is a problem, however. Considering scheme (12), the product state ratio of $m=2/m=3$ should be predictable, since the rate constants are known, and this prediction is not in accord with experiments. The time-dependent buildup of the population of $I_2(v'-2)$ divided by the initial population of excited $I_2Ne_2(v')$ clusters, $P(t)$, is given by

$$P(t)=\frac{k_1^{VP}}{K_1}-\frac{k_1^{VP}k_2^{VP}}{k_2^{VP}-K_1}\left\{\frac{\exp[-K_1 t]}{K_1}-\frac{\exp[-k_2^{VP}t]}{k_2^{VP}}\right\}. \tag{14}$$

In Eq. (13), the signal represents $P(t)$ times a constant factor K_1/k_1^{VP}, which does not alter the temporal behavior. Letting $t\rightarrow\infty$ in Eq. (14) leads to the following product state ($v_i' - 2$) population:

$$P=\frac{k_1^{VP}}{K_1}=\frac{k_1^{VP}}{k_1^{VP}+k^r}. \tag{15a}$$

As only two channels are considered, the sum of P and the product state ($v_i' - 3$) population, Q, must be one, yielding

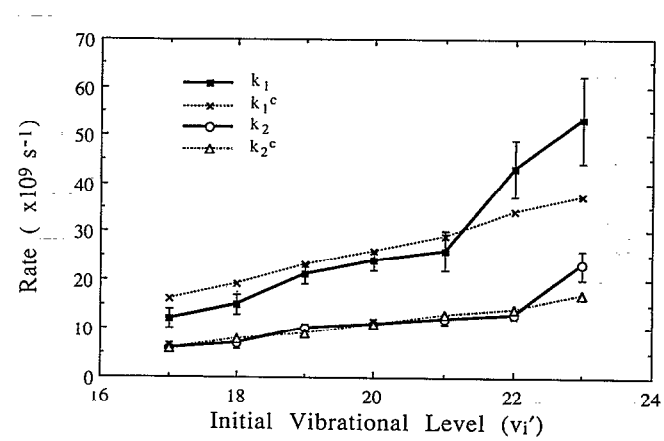

FIG. 4. The experimental rates, k_1 and k_2, and the theoretical rates, k_1^c and k_2^c, vs the initially prepared vibrational state v_i'. A description of the theoretical model is given in the text.

$$Q=\frac{k^r}{K_1}=\frac{k^r}{k_1^{VP}+k^r}. \tag{15b}$$

Thus the branching ratio for the two channels is simply

$$\frac{\text{probability}(m=2)}{\text{probability}(m=3)}=\frac{k_1^{VP}}{k^r}. \tag{16}$$

The time constants we obtained for the first step (see Tables I and II) would imply that the $m=3$ channel is relatively unimportant. As discussed above, the first step in I_2Ne_2 is about twice as fast as the corresponding VP in I_2Ne, which implies that k^r should be negligible. This finding would be in contradiction with our detection of nascent I_2 in the $m=3$ channel and the results of Levy and coworkers[4] who found that the branching into the channels $m=2$ and $m=3$ occurs with about equal probability for $v_i'=21,22$. It is not expected that this branching ratio will change by orders of magnitude when going to the other v_i' levels under study. Thus according to Eq. (16), k^r and k_1^{VP} should be about equal in magnitude and K_1 should have a value about four times as large as the corresponding VP rate constant of I_2Ne [see Eqs. (10) and (11)].

The discrepancy can be understood by considering a slight revision of the above scheme (12). The local mode picture restricts the extent of the energy flow from the I_2 stretch coordinate into the reactive vdW coordinates. What must also be considered, however, are the cluster modes, taking into account the fact that the motions of the atoms are correlated. I_2Ne_2 now becomes a "large" system with six modes. These clusters are quite "floppy" with low-frequency, large amplitude modes. In fact, Janda's group[24] described Cl_2He_2 as a liquidlike cluster, and using the instantaneous normal mode analysis, Adams and Stratt[25] obtained a phonon spectrum for Ar_2. Therefore, instead of the two local mode reaction coordinates, R_1 and R_2, for the two I_2–Ne distances, we consider the reactive and nonreactive coordinates with possible IVR to either of them (see Fig. 1).

For I_2Ne ($n=1$) there is only one VP pathway. For I_2X in general, e.g., X=Ar, there is a possibility for IVR preceding VP, depending on the Δv energy release relative to the energy of the vdW bond. In the situation depicted in Fig. 1 for I_2Ar, a coherent pulse can prepare a coherent superposition of states and energy can flow (IVR) first from $|v,0\rangle$, the zero-order state, which carries some oscillator strength, to $|v-1,l\rangle$ and/or $|v-2,l\rangle$, which in turn undergo VP to the $|v-3,\epsilon\rangle$ continuum. If, on the other hand, an eigenstate is prepared, these sequential dynamics will not be observed and VP from a mixed state $\alpha|v,0\rangle+\beta|v-1,l\rangle+\gamma|v-2,l\rangle$ will be observed. Such a dynamical behavior of coherent energy redistribution has been observed in IVR experiments, even in large molecules.[17,18] (Incoherent preparation of states can lead to averaging out of these IVR resonance effects[17,26]). Janda's group[27] has shown the importance of this issue of the preparation of state in Cl_2Ar and Gray[28] has found (theoretically) such an IVR process in I_2Ar. For the I_2Ne cluster (Fig. 1), the energetics ($\Delta v=-1$ gives $<100\ \text{cm}^{-1}$, $D_0\sim 66\ \text{cm}^{-1}$) do not allow for such a mechanism, in contrast to I_2Ar or Cl_2Ar where there are bound intermediate ($v-k$) states [see (II), Figs. 6 and 7 and here, Fig. 1). For I_2Ar, $\Delta v=-1$ gives $<100\ \text{cm}^{-1}$, $D_0\sim 235\ \text{cm}^{-1}$ (Ref. 11); for Cl_2Ar, $\Delta v=-1$ gives $<200\ \text{cm}^{-1}$, $D_0\sim 178\ \text{cm}^{-1}$ (Ref. 29).

In the case of I_2Ne_2 (or larger clusters) reactive (mixed) modes are not necessarily pure local (l) modes and their energetics may allow for such a behavior. Some can have the required dissociation energy. We will consider IVR in these clusters to be direct, if such modes form intermediate bound or quasibound levels for the initial state to interact with. Thus IVR could preceed direct VP and this is now evident in a number of cases, e.g., IVR prior to isomerization[30] and IVR prior to VP in stilbene vdW clusters.[22]

Let us now expand on this description and consider I_2Ne_2. The correlated cluster modes (as opposed to local modes) with high-lying energy levels can serve as accepting modes for one quantum of the I_2 stretch from the initial state $|v,0\rangle$. Some of these cluster modes will contain the reaction coordinate(s), i.e., be strongly coupled to either or both of the energetically accessible translational continua (loss of one Ne atom). Other modes will not efficiently couple to the reaction coordinates and thus be able to "trap" one quantum of the I_2 stretch and possibly undergo further coupling to other cluster modes. In a simplified picture, in analogy to an ABA potential hypersurface, one may think of a reactive mode as containing an antisymmetric stretch motion of the Ne atoms with respect to the center of the I_2 bond, which is connected to the continuum by "overstretching" to one side. A nonreactive mode may, for example, contain the corresponding symmetric stretch motion of the two Ne atoms and be able to trap one quantum of the I_2 stretch (resonance). A (symmetric) cluster mode involving both rare gas atoms can also explain a nonvanishing probability for multiple continua access (dissociation of two Ne atoms at one in a two quantum process) and formation of some Ne_2 as calculated in Ref. 21.

In this total mode picture, the first step of the I_2Ne_2 cluster dynamics will involve IVR into either reactive modes (k^{rr}) or nonreactive modes (k^{nr})

$$I_2Ne_2(v_i')\begin{cases}\xrightarrow{k^{rr}} I_2Ne_2(v_i'-1,r)\\ \xrightarrow{k^{nr}} I_2Ne_2(v_i'-1,nr)\end{cases}. \tag{17}$$

(The asterisk on I_2 used previously has been dropped for simplicity). This would then give the branching into the reactive (r) and nonreactive (nr) channels. If the reactive mode is excited to an energetically high lying level, dissociation into the continuum could occur extremely fast (k_{diss}) leaving I_2Ne, which subsequently could undergo normal VP as in I_2Ne excited into the B state (I). We note that the system is no longer one-dimensional in R and a highly excited and "bound" reactive mode can "see" a translational continuum, the second dimension. Again, the situation is reminiscent of ABA systems on electronic (here, vibrational) potential hypersurfaces with a trajec-

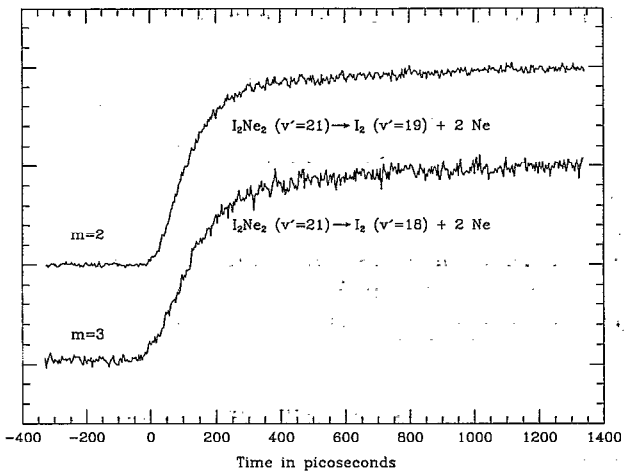

FIG. 5. Two I_2Ne_2 ($v_i' = 21$) transients showing the m dependence of VP.

tory at the saddle point bound in the symmetric coordinate and unbound in the antisymmetric coordinate.

Following IVR from the v_i' state to the $(v_i' - 1,r)$ state, the process can be written as

$$I_2Ne_2(v_i'-1,r) \xrightarrow{k_{\text{diss}}} I_2Ne(v_i'-1) \xrightarrow{k^{VP}} I_2(v_i'-2), \quad (m=2) \tag{18}$$

which is similar in form to Eq. (12), but now the branching of $m=2/m=3$ can be accounted for by IVR. Considering IVR [precursor in Eq. (18)], the buildup of nascent I_2 according to Eq. (18) is a triple exponential. However, the dissociative step is expected to be extremely fast (< 10 ps) and given our experimental time resolution, a double exponential buildup is predicted. k^{rr} strongly depends on v_i' due to the anharmonicity of the I_2 stretch; the energy-gap between this mode and the accepting (low frequency) cluster modes will become smaller and thus the coupling will increase with v_i'. k^{rr} is similar to k^{VP} of the first step with two differences. First, to break the I_2–Ne bond, the IVR process of k^{rr} is followed by the very fast dissociation process and the "rate determining step" is the initial v_i' to $v_i' - 1$ process. Second, the coupling is from the I_2 stretch to now a "mixed" reactive mode and k^{VP} should be somewhat different from $2k_0^{VP}(1)$. From Table II, we see differences as large as 25%.

The second step in the effective double exponential of Eq. (18) should then reflect VP of I_2Ne [see (I) and Table II] from $I_2Ne(v_i' - 1)$ to yield $I_2(v_i' - 2)$. These predictions are in good agreement with our observations (see Table II).

A consequence of the above analysis is a prediction about the $m=3$ channel. For this channel, k^{nr} is a key for involving the nonreactive modes. As the energy of one quantum of the I_2 stretch is trapped in the cluster modes, further mode coupling to other cluster modes is possible. A second quantum of the I_2 stretch can then be transferred to the cluster modes, either into the reactive channels or the nonreactive channels. Transfer into the reactive channels would lead to the subsequent process described above. Transfer into nonreactive modes would leave the cluster hot and (perhaps) statistical dissociation (evaporation) is possible. The number of redistribution and evaporation pathways would increase with cluster size as more nonreactive modes would become available for energy storage and higher m quantum channels would become dominant as observed for larger clusters.[4]

The $m=3$ channel in I_2Ne_2 should show a multiple-exponential behavior and be effectively slower than the $m=2$ channel. The overall rate will depend on v_i' through k^{nr} as discussed for the reactive channel. The branching will be determined by k^{rr}/k^{nr}, and according to the above discussion both rate constants will be about equal. This is plausible as both describe similar processes, vibrational/rotational energy redistribution.

An example of our results for the $m=3$ channel is displayed in Fig. 5 which shows a pair of transients for $v_i' = 21$; the top one corresponds to the $m=2$ channel of I_2Ne_2, whereas the bottom one is for $m=3$. The results indicate that the kinetics for both channels are very different. The $m=3$ channel shows a significantly slower overall rate than the $m=2$ channel (for $m=2$, "τ"$=103$ ps± 4 ps, while for $m=3$, "τ"$=145$ ps± 11 ps; the transients were "fitted" to single exponential rise functions). Hence, it can be concluded that the higher m quantum channels of VP in I_2Ne_n clusters are slower with respect to the lower m quantum channels, consistent with the above model of reactive and nonreactive division of the cluster modes. Further femtosecond studies are planned in order to map out the early time behavior of this system and test the details of this picture, particularly the importance of coherence and the separation of the intermediates.

Calculations of the vibrational predissociation of I_2Ne_2 have been performed by two groups, Schatz, Buch, Ratner, and Gerber (SBRG)[31] and Garcia-Vela, Villarreal, and Delgado-Barrio (GVD).[21] Both groups performed their calculations for the $v_i' = 28$ level. The calculations of SBRG were restricted to I_2Ne_2 in a collinear configuration. These authors did quasiclassical trajectory (QCT) calculations as well as classical time-dependent self-consistent field (TDSCF) calculations which agreed fairly well with each other. SBRG obtained the lifetimes from a simple two-step VP process. For each step, a single exponential decay was assumed.

The QCT calculations yielded a lifetime of 5 ps for the first step and 13 ps for the second step. The fact that the first step was found to be more than twice as fast as the second step (cp. the simple estimate for a two-step VP in Sec. III A) was interpreted in terms of an acceleration of the first step, mediated by I_2 recoiling from the second Ne atom and hitting the first Ne atom hard, such that it leaves the cluster faster than if no second Ne atom was present. SBRG also calculated the action losses during VP whose values divided by $\hbar$ can be related to the number of I_2 stretch quanta lost. For the first step, SBRG found action losses of $2.29\,\hbar$ corresponding to nascent $I_2Ne(v_i' - 2)$. For the second step, they observed non-transient fragments I_2Ne losing $0.98\,\hbar$ [corresponding to the product $I_2(v_i' - 3)$] which have the above quoted lifetime of 13 ps and transient fragments I_2Ne which dissociate immediately

with an action loss of 0.002 $\hbar$ [corresponding to the product $I_2(v_i' - 2)$]. Thus according to SBRG, the $m=2$ channel should be almost single exponential and correspond to a double continuum process where both Ne atoms are lost more or less simultaneously.

The $m=3$ channel should then show double-exponential kinetics corresponding to sequential bond breakage. We also observe a slow down of the first step with respect to the second, which, however, can easily be explained even by the simple considerations discussed in Sec. III A (the simple two-step process). The first step involves twice the rate of I_2Ne prepared in v_i' and the second rate is the one for VP of I_2Ne prepared in $v_i' - 1$. As shown in (I), VP of I_2Ne increases with increasing v_i', thus the first step must be faster than twice the second step. An impulsive picture using a collinear geometry is not necessary to explain these results, especially since the structure of I_2Ne_2 is most likely nonlinear as discussed in Ref. 4. I_2He is known to be nonlinear, see Ref. 32 and (II). As the kinetics we observe are at least double exponential, a simultaneous bond breakage as inferred from the calculations of SBRG does not seem to play a major role for the $m=2$ channel.

GVD,[21] on the other hand, performed QCT calculations on the first VP step of I_2Ne_2 ($v_i' = 28$) in a nonlinear configuration confined to the following motions: I_2 stretch, Ne center-of-mass (I_2) stretch, and van der Waals bend along a plane perpendicular to the I_2 moiety. GVD calculated a VP time of 7.36 ps for the first step, approximately 1.5 times longer than the result obtained by SBRG. In addition, this lifetime is 2.85 ps larger than expected by Eq. (10). Thus GVD observe a slow down. They interpret this slow down in terms of IVR processes occurring in larger clusters due to the presence of accepting cluster modes. This interpretation is consistent with our model discussed above, however, the slow down they observe is quite large compared to our experimental findings (we observe a significant slow down only for $v_i' = 17,18$). GVD did not report any action losses during VP for their calculations; a distinction between the $m=2$ and the $m=3$ channel does not seem to have been made in obtaining the lifetimes. Thus the calculated slow down could be exaggerated by the fact that both channels are somehow mixed in these calculations, and the $m=3$ channel leads to longer lifetimes. GVD also found some probability for double continuum transitions (loss of two Ne atoms at once) and formation of Ne_2 which is in line with our cluster mode discussion above.

C. The I_2Ne_n ($n=3,4$) clusters

In order to compare the dynamics of the various clusters I_2Ne_n, we have introduced an effective overall rate of VP as, thus far, we have only probed the nascent I_2 fragment in the dominant channel and the number of possible pathways increase with n. The simplest way of defining such an effective rate is by fitting all measured transients to single exponential rise functions, which leads to an effective overall rate constant k_{eff}. Such a fit cannot, of course, describe any subtleties of the detailed kinetics, but should at least provide a rate determining step to the transition from the initially excited metastable cluster state v_i' to the product state v_f' of nascent I_2. The k_{eff} values along with the corresponding times τ_{eff} are listed in Table III. Values which are calculated from Eq. (10) and then fitted to a single exponential rise ($k_{\text{eff}}^c, \tau_{\text{eff}}^c$) are also given. These values refer to a simple n-step sequential bond breakage and the necessary data for VP of I_2Ne are taken from (I). Figure 6 shows the experimental rate constants k_{eff} vs v_i' for the different clusters. For I_2Ne_2, both the $m=2$ and the $m=3$ channels are shown. Included for comparison are the results for I_2Ne from Paper (I). The calculated values k_{eff}^c are also plotted in this figure.

In Table III(a), the results for I_2Ne are shown for comparison, and in Table III(b), the data for I_2Ne_2 ($m=2$ channel) are presented. As discussed in Sec. III B, the calculated and observed values agree well and do not show evidence for a significant slow down of the rates, except for $v_i'=17,18$.

Table III(c) shows the corresponding results for I_2Ne_2 ($m=3$ channel). All rates measured for this channel are significantly smaller than the calculated ones. From the table and Fig. 6, it can be seen that a simple two-step mechanism is not appropriate in describing the $m=3$ channel dynamics. The slow down of the measured rates with respect to those calculated is evident, and can be understood using the concepts discussed above. As with I_2Ne_2, the slow down becomes more significant with lower v_i'.

In Table III(d), the results for I_2Ne_3 ($m=4$ channel) and for I_2Ne_4 ($m=5$ channel) are shown. The trend observed in I_2Ne_2 is continued for the higher clusters; the slow down of the measured rates with respect to those calculated implies that IVR steps precede the actual bond breakage and overall VP becomes relatively slow (Fig. 6). Increasing the cluster size provides an increasing density of bath states, making IVR processes increasingly efficient, but the time spent for enough energy to get into the reactive vdW coordinates becomes longer, as would be predicted by statistical theories when ρ increases. In addition, higher VP channels are observed[4] with increasing cluster size; more and more energy is dissipated into the internal cluster modes. Furthermore, as the number of bath states of the intermediate fragments becomes larger with increasing size of the parent cluster, additional IVR processes within these fragments lead to an efficient slow down of the overall VP rate.

QCT calculations for the higher clusters I_2Ne_n (n up to 9) have also been performed for the first step of VP ($v_i' = 28$) by GVD.[21] Comparing with the simple n-step process [cp. Eq. (10)], the authors found decreasing rates with increasing cluster size which they interpreted in terms of increasing IVR due to the increasing number of storage modes. These results are in line with our observations for the overall rates of the higher clusters. It should be mentioned, however, that GVD did not distinguish between the different channels of VP; hence, their lifetime results should be viewed as channel averaged.

Since IVR increases with n, the larger clusters may be described by a statistical $k(E)$ for the evaporation of Ne

TABLE III. The effective rate and time constants measured for a number of I_2Ne_n systems: $I_2Ne_n(v_i') \rightarrow I_2(v_f') + n\,Ne$.

v_i'	v_f'	τ_{eff} (ps)[a]	τ_{eff}^c (ps)[a]	k_{eff} (10^9 s^{-1})	k_{eff}^c (10^9 s^{-1})
a) I_2Ne, $m=1$[b]					
13	12	216±16	216±16	4.6±0.4	4.6±0.4
14	13	196±12	196±12	5.1±0.3	5.1±0.3
15	14	182±20	182±20	5.5±0.6	5.5±0.6
16	15	160±15	160±15	6.3±0.6	6.3±0.6
17	16	126±12	126±12	7.9±0.8	7.9±0.8
18	17	107± 9	107± 9	9.3±0.9	9.3±0.9
19	18	87± 4	87± 4	11.5±0.9	11.5±0.9
20	19	78± 4	78± 4	12.8±1.0	12.8±1.0
21	20	69± 6	69± 6	14.5±0.7	14.5±0.7
22	21	58± 3	58± 3	17.2±0.9	17.2±0.9
23	22	53± 3	53± 3	18.9±1.0	18.9±1.0
b) I_2Ne_2, $m=2$					
17	15	209±19	184	4.8±0.5	5.4
18	16	172±10	147	5.8±0.4	6.8
19	17	124± 6	124	8.1±0.4	8.1
20	18	112± 4	103	8.9±0.4	9.7
21	19	103± 4	92	9.7±0.4	10.9
22	20	81±10	80	12.3±1.6	12.5
23	21	51± 3	69	19.6±1.2	14.5
c) I_2Ne_2, $m=3$					
19	16	230±30	124	4.3±0.6	8.1
20	17	162±13	103	6.2±0.5	9.7
21	18	145±11	92	6.9±0.6	10.9
22	19	114± 7	80	8.8±0.6	12.5
d) I_2Ne_3, $m=4$					
20	16	173±18	129	5.8±0.6	7.8
21	17	156± 9	107	6.4±0.4	9.3
22	18	130± 7	95	7.7±0.5	10.5
23	19	118± 7	84	8.5±0.5	11.9
e) I_2Ne_4, $m=5$					
22	17	176	109	5.7	9.2

[a]The values of τ_{eff} reported in this table were obtained by fitting the measured transients to a single exponential function convoluted with a 40 ps Gaussian system response. The value reported for τ_{eff} is the average of a number of transients; the reported errors are one standard deviation. The values of τ_{eff}^c are obtained from fitting a calculated transient for a n-step sequential dissociation [based on the results for I_2Ne and using Eq. (10)] to a single exponential rise.

[b]For I_2Ne we have a true single exponential rise, see (I), and $\tau_{eff} = \tau_{eff}^c \equiv \tau$.

atoms. One can use standard RRKM theory, phase space theory (PST) or the Engelking model[33] to obtain $k(E)$. The problem, however, is that even in the simplest RRK expression

$$k^n(E) = \nu \left[\frac{E - E_0^n}{E}\right]^{s_n - 1}, \tag{19}$$

one needs to know the effective number of modes s_n for the different clusters. The energy threshold E_0^n and the frequency factor ν are easier to obtain. The transition state should be close to the product (exit channel), and PST may be more adequate. It is interesting to note that for $n=1$ [ν taken to be the vdW stretch frequency[11] corresponding to 25 cm^{-1}, $E_0 = D_0 = 66$ cm^{-1}, $E = 91$ cm^{-1} ($v_i' = 20$, $\Delta v = -1$)], we obtain $k(E) = (18\text{ ps})^{-1}$ when the I_2 stretch is included ($s_n = 3$), and $k(E) = (5\text{ ps})^{-1}$ when the I_2 stretch is excluded ($s_n = 2$).

For any serious estimate of $k(E)$, the density of states must be considered carefully in such "floppy" systems. Amar has addressed these points in his calculation of evaporation rates in $Br_2^-(CO_2)_n$. Since the rates are measured and the rare gas/I_2 potential parameters have been deduced, the neutral clusters I_2Ne_n should be ideal systems to compare theory with experiments in hope of quantifying the nature of the modes involved in IVR, VP, and evaporation.

IV. CONCLUSIONS

In this paper, we presented real-time studies of the picosecond fragmentation and evaporation in the I_2Ne_n ($n = 2$–4) clusters. We have examined the pathways for direct vibrational predissociation (VP) and for the onset of energy redistribution (IVR) as the cluster size increases. The elementary VP process and its dependence on the quantum number of the $I_2(v_i')$ stretch has been studied. The process can be understood as a direct coupling, employing the repulsive force between I_2 and Ne, between the I_2 stretch (in v_i') and the continuum of states of ($v_i' - 1$).

As the cluster size increases, we observe the onset of IVR with the overall rate of I_2 appearance decreasing with n. IVR accesses reactive and nonreactive modes and this

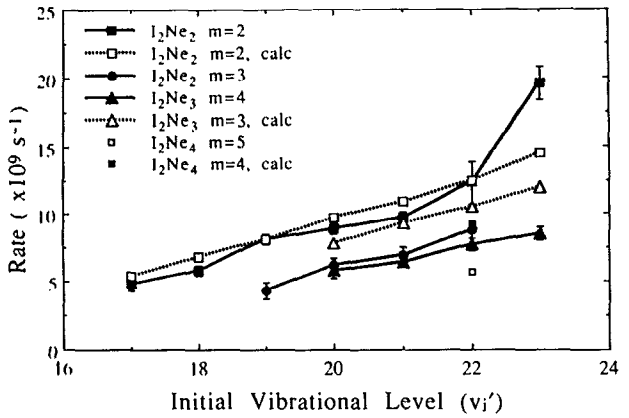

FIG. 6. The v_i' dependence of the effective reaction rates for a number of I_2Ne_n clusters. A description of the effective rates is presented in the text.

leads to direct fragmentation or statistical-type evaporation. Similar to previous IVR studies in real time, the question of the preparation of state becomes important in establishing IVR as a precursor to VP. The evidence comes from careful examination of I_2Ne_2 steps whose transient results show a double exponential buildup of nascent iodine. With this simple model, we can understand the rates, their dependence on v_i', and the product state distributions.

As n increases further, the situation is more complex, and instead of analyzing all steps, we introduce an effective rate which slows down (experimentally) as n increases and v_i' decreases. Although IVR increases with n (and this leads to more channels "m" in nascent iodine with $m > n$), the statistical "average" rate decreases as energy takes more time to find the reaction coordinate (larger effective density of states).

These halogen–rare gas systems are quite interesting and there remain a number of theoretical and experimental problems to be addressed. Experiments on a shorter time scale are in progress. Also of interest are comparisons with results for the same system, but at high rare gas densities.[34,35] Little is known about the theoretical predictions of the structure and dynamics for large n, and hopefully with the aid of experiments, theoretical studies can quantify the behavior with v_i' and n. In a following paper, we focus on one such question, the role of direct excitation to the reaction coordinate.[36]

Note added in proof. Studies of the elementary nuclear motion on the femtosecond time scale has been reported recently for iodine in large argon clusters.[37]

ACKNOWLEDGMENT

This work was supported by a grant from the National Science Foundation (DMR).

[1] D. M. Willberg, M. Gutmann, and A. H. Zewail, J. Chem. Phys. **96**, 198 (1992).
[2] M. Gutmann, D. M. Willberg, and A. H. Zewail, J. Chem. Phys. **97**, 8037 (1992).
[3] W. Sharfin, K. E. Johnson, L. Wharton, and D. H. Levy, J. Chem. Phys. **71**, 1292 (1979).
[4] J. E. Kenny, K. E. Johnson, W. Sharfin, and D. H. Levy, J. Chem. Phys. **72**, 1109 (1980).
[5] B. A. Swartz, D. E. Brinza, C. M. Western, and K. C. Janda, J. Chem. Phys. **88**, 6272 (1984).
[6] S. R. Hair, J. I. Cline, C. R. Bieler, and K. C. Janda, J. Phys. Chem. **90**, 2935 (1989).
[7] J. C. Drobits and M. I. Lester, J. Chem. Phys. **86**, 1662 (1987).
[8] L. Khundkar and A. H. Zewail, Annu. Rev. Phys. Chem. **41**, 15 (1990), and references therein.
[9] M. L. Alexander, N. E. Levinger, M. A. Johnson, D. Ray, and W. C. Lineberger, J. Chem. Phys. **88**, 6200 (1988); D. Ray, N. E. Levinger, J. M. Papanikolas, and W. C. Lineberger, *ibid.* **91**, 6533 (1989); J. M. Papanikolas, J. R. Gord, N. E. Levinger, D. Ray, V. Varsa, and W. C. Lineberger, J. Phys. Chem. **95**, 8028 (1991).
[10] F. G. Amar and B. J. Berne, J. Phys. Chem. **88**, 6720 (1984); L. Perera and F. G. Amar, J. Chem. Phys. **90**, 7354 (1989); F. G. Amar and L. Perera, Z. Phys. D **20**, 173 (1991); F. G. Amar and S. Weerasinghe, in *Mode Selective Chemistry, Proceedings of the 24th Jerusalem Quantum Chemistry Symposium*, edited by B. Pullman and J. Jortner (Kluwer, Amsterdam, 1991).
[11] J. A. Blazy, B. M. DeKoven, T. D. Russell, and D. H. Levy, J. Chem. Phys. **72**, 2439 (1980).
[12] D. H. Levy, Adv. Chem. Phys. **47**, part I, 323 (1981).
[13] Program written by M. Gruebele of this group.
[14] P. R. Bevington, *Data Reduction and Error Analysis for the Physical Sciences* (McGraw-Hill, New York, 1969), p. 204.
[15] M. E. Kellman, Chem. Phys. Lett. **76**, 225 (1980).
[16] Only the continuum states are assumed to be energy normalized [see Eq. (4) in (I) and Eq. (8) here where ρ does not appear explicitly). Equation (7) is for discrete states and thus the density of states ρ appears explicitly.
[17] P. M. Felker and A. H. Zewail, Adv. Chem. Phys. **70**, part I, 265 (1988), and references therein.
[18] P. M. Felker and A. H. Zewail, J. Chem. Phys. **82**, 2975 (1985); D. R. Demmer, J. W. Hager, G. W. Leach, and S. C. Wallace, Chem. Phys. Lett. **136**, 329 (1987); X. Song, C. W. Wilkerson, Jr., J. Lucia, S. Pauls, and J. P. Reilly, *ibid.* **174**, 377 (1990); P. G. Smith and J. D. McDonald, J. Chem. Phys. **92**, 1004 (1990); J. M. Smith, C. Lakshminarayan, and J. L. Knee, *ibid.* **93**, 4475 (1990); A. J. Kaziska and M. R. Topp, Chem. Phys. Lett. **180**, 423 (1991)
[19] See Ref. 17 for the correspondence and the limits between the quantum treatment of IVR and the kinetic equation approach.
[20] A superscript VP is used for k^{VP} [instead of k_{VP} as in (I)] because of the multiple steps involved in the VP processes discussed here; these steps are labelled by subscripts, for example, k_1^{VP}.
[21] A. Garcia-Vela, P. Villarreal, and G. Delgado-Barrio, J. Chem. Phys. **94**, 7868 (1991).
[22] D. H. Semmes, J. S. Baskin, and A. H. Zewail, J. Chem. Phys. **92**, 3359 (1990).
[23] M. Dantus, R. M. Bowman, M. Gruebele, and A. H. Zewail, J. Chem. Phys. **91**, 7437 (1989); in this case, both channels are possible: Hg +I+I and HgI+I; the propensity is determined by the topology of the potential energy surface and the time scale of the dynamics.
[24] W. D. Sands, C. R. Bieler, and K. C. Janda, J. Chem. Phys. **95**, 729 (1991).
[25] J. E. Adams and R. M. Stratt, J. Chem. Phys. **93**, 1332 (1990).
[26] A. H. Zewail, Ber. Bunsenges. Phys. Chem. **89**, 264 (1985).
[27] N. Halberstadt, J. A. Beswick, O. Roncero, and K. C. Janda, J. Chem. Phys. **96**, 2404 (1992).
[28] S. K. Gray, Chem. Phys. Lett. (in press).
[29] D. D. Evard, J. I. Cline, and K. C. Janda, J. Chem. Phys. **88**, 5433 (1988).
[30] J. A. Syage, P. M. Felker, and A. H. Zewail, J. Chem. Phys. **81**, 4706 (1984).
[31] G. C. Schatz, V. Buch, M. A. Ratner, and R. B. Gerber, J. Chem. Phys. **79**, 1808 (1983).
[32] R. E. Smalley, L. Wharton, and D. H. Levy, J. Chem. Phys. **68**, 671 (1978).
[33] P. C. Engelking, J. Chem. Phys. **85**, 3103 (1986); **87**, 936 (1987).
[34] M. Dantus, R. M. Bowman, A. Mokhtari, and A. H. Zewail, J. Photochem. Photobiol. A **62**, 301 (1992).
[35] Y. Yan, R. M. Witnell, K. R. Wilson, and A. H. Zewail, Chem. Phys. Lett. **193**, 402 (1992).
[36] D. M. Willberg, M. Gutmann, E. E. Nikitin, and A. H. Zewail, Chem. Phys. Lett. (in press).
[37] E. Potter, Q. Liu, and A. H. Zewail, Chem. Phys. Lett. (in press).